

Review

# Effect of Non-Homogeneous Soil Characteristics on Substation Grounding-Grid Performances: A Review

Navinesshani Permal<sup>1,\*</sup>, Miszaina Osman<sup>1</sup>, Azrul Mohd Ariffin<sup>1</sup> and Mohd Zainal Abidin Ab Kadir<sup>2</sup>

<sup>1</sup> Institute of Power Engineering, Universiti Tenaga Nasional, Jalan IKRAM-UNITEN, Kajang 43000, Selangor, Malaysia; miszaina@uniten.edu.my (M.O.); azrula@uniten.edu.my (A.M.A.)

<sup>2</sup> Centre for Electromagnetic and Lightning Protection Research (CELP), Advanced Lightning, Power and Energy Research Centre (ALPER), Universiti Putra Malaysia, Seri Kembangan 43400, Selangor, Malaysia; mzk@upm.edu.my

\* Correspondence: nesshani@yahoo.com

**Abstract:** Designing an effective grounding system for AC substations needs predetermination of ground resistance and ground potential distribution caused by fault current's presence in the ground. Therefore, it is necessary to have a suitable grounding grid structure in the soil properties in which the grid is buried. Though the soil composition where the grounding grid is located is typically non-homogeneous, the soil is often presumed to be homogeneous due to the complexities of grounding system analysis in non-homogeneous soil. This assumption will lead to inaccuracies in the computation of ground resistance and ground potentials. Although extensive research has been done on non-homogeneous soil structure, comprehensive literature on grounding system performance in non-homogeneous soil is yet to be reviewed. Thus, this paper reviews the effect of non-homogeneous soil on the grounding system, with different soil characteristics in horizontal and vertical two-layer soil structure and the horizontal three-layer soil structure. In addition, the effect of design parameters on the grounding performance in non-homogeneous soil conditions for non-transient fault conditions is also studied. The significance of this study is that it provides a comprehensive review of grounding performance as grounding design changes and their effects as soil layers and their corresponding features change. This knowledge will be useful in developing safe grounding designs in non-homogeneous soil.

**Keywords:** homogeneous soil; non-homogeneous soil; two-layer soil; three-layer soil; soil characteristics; substation grounding



**Citation:** Permal, N.; Osman, M.; Ariffin, A.M.; Abidin Ab Kadir, M.Z. Effect of Non-Homogeneous Soil Characteristics on Substation Grounding-Grid Performances: A Review. *Appl. Sci.* **2021**, *11*, 7468. <https://doi.org/10.3390/app11167468>

Academic Editor: Eduardo Ferreira da Silva

Received: 5 July 2021

Accepted: 1 August 2021

Published: 14 August 2021

**Publisher's Note:** MDPI stays neutral with regard to jurisdictional claims in published maps and institutional affiliations.



**Copyright:** © 2021 by the authors. Licensee MDPI, Basel, Switzerland. This article is an open access article distributed under the terms and conditions of the Creative Commons Attribution (CC BY) license (<https://creativecommons.org/licenses/by/4.0/>).

## 1. Introduction

Generally, the earth is made of multiple compositions with distinct soil properties. The electric constants of soil, such as permittivity ( $\epsilon$ ) and resistivity ( $\rho$ ) depend on the type of soil such as sand, limestone, clay, or gravel [1–7]. The effect of various electric constants of soil on the grounding performances has been tested through many types of research. For example, authors in [8–14] explained the fundamental knowledge on soil resistivities and their effects on the performances of grounding systems; the effects of grounding system design in two-layer soil are well presented in [15–22]; the grounding system responses in multilayer soil with different resistivities are also explained in [18,23–26], and algorithms developed to evaluate apparent soil resistivity [27–34]. These values typically differ on the surface of the soil from layer to layer, which may affect the effectiveness of the touch and step potentials and grounding resistance.

For example, the effect on grounding resistance is more significant when there are large differences between the soil layer resistivity. The nature and structure of soil available such as sand, gravel, etc., determines the soil resistivity. Although some fundamental information and equations on two-layer soil structure are available—most standards and regulations specify grounding grid designs based on homogenous soil conditions.

Homogeneous soil conditions are used as an input to the measurement of safety threshold values in most substation grounding system safety assessments and design protocols. Authors in [35–37] examined the performance of grounding systems under homogenous soil conditions. However, due to the difficulty of the numerical computations required, multiple soil layers are usually ignored when designing a grounding system. The substation grounding design will be inaccurate if non-homogeneous soil conditions are not taken into account during the grounding designing phase [25]. Thus, as a result, this study offers a comprehensive review of the effects of non-homogeneous soil structure (two and three-layered horizontal soil and two-layer vertical soil), with various characteristics on grounding system performance.

## 2. Effect of Horizontal Two-Layer Soil Characteristics on Grounding System Performances

### 2.1. Depth of Grid Buried in a Two-Layer Soil

Apart from grounding grid design parameters, the depth of the grid buried in the soil, especially in the two-layer soil model [19,38–41] has a significant impact on the protection of a grounding system. Grid burial depths are generally in the range of 0.5 m to 1.5 m, or 2.0 m to 2.5 m in some cases, according to IEEE 80 [42]. Generally, increasing the depth of the grounding grid buried into soil reduces the grid impedance and ground potentials in homogeneous soil. On the other hand, the behavior of a grounding system would be different when the depth of the grid increases in a two-layer soil structure, which will be discussed in this section.

An example has been adapted from [40] to show the Ground Potential Rise (GPR) performances as the depth of the grid is increased. The GPR is obtained for  $30\text{ m} \times 35\text{ m}$  area, the top layer's soil resistivity is  $37.82\ \Omega\text{m}$  ( $\rho_1$ ) with 5.15 m depth ( $h$ ), the deep layer soil resistivity is  $120.42\ \Omega\text{m}$  ( $\rho_2$ ) with infinite depth, the grid is attached with 3 m vertical rod length as shown in Figure 1. The figure shows 4 different scenarios (A, B, C, D); with the presence of 3 m ground rods and without the rods. Cases A and C show the grounding grid with vertical rods; whereas in the case of A, the top layer soil is less resistive than the bottom layer and vice versa in case C. Cases B and D show the grounding grid without vertical rods; wherein case B, the top layer soil is less resistive than bottom layer and vice versa in case D.

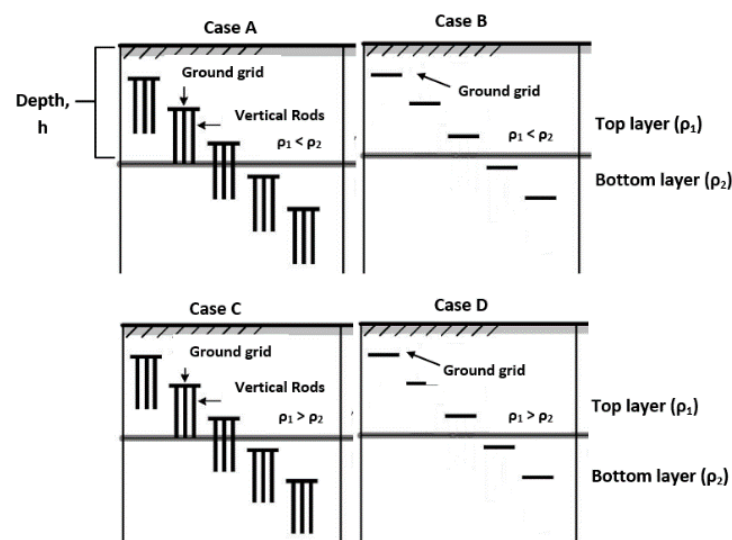


Figure 1. Visual representation of cases A, B, C, and D.

Table 1 summarizes the findings such that increasing the depth of the grid in high resistive bottom layer soil increases the GPR value [40]. The bottom layer's high resistivity allows more current flow towards the upper layer's lower resistivity, raising the ground surface potential. In the low resistive top layer soil, however, increasing the grid depth

decreases the GPR value. A number of vertical rods attached to the main grounding grid help to enhance a grounding grid's safety by reducing the GPR value. Therefore, it is also evident that the GPR is lower for a grounding system with vertical rods than a grounding system without vertical rods.

**Table 1.** GPR performances for each case.

Case	GPR
A	Reduces until it reaches the border of the top layer and increases after the grid enters the bottom layer with high resistivity.
B	The same trend as case A, but the GPR values are higher than case A.
C	Reduces significantly as the depth of the grid buried rises, particularly after the border of the top layer.
D	The same pattern as in case C but higher GPR values than case C.

## 2.2. The Resistivity and Depth of Top Layer Soil

A grounding system for a substation in a two-layer soil structure must be carefully designed for safety purposes. The IEEE 81-2012 standard [43] explains how a grid buried in a non-homogeneous soil layer with a different soil resistivity affects its performance. The soil resistivity in each layer, as well as the height of the soil's top layer, influence the grid's behavior. This study is crucial because it allows the designer to anticipate the grid impedance pattern and determine the length of additional vertical rods if needed to enhance the grounding safety, depending on the top soil layer height.

A sudden transformation in resistivity that occurs at the borders of the soil layer is denoted in Equation (2) as a reflection coefficient (K). Equations (1) and (2) [18] are used to calculate the two-layer soil's parameters where K signifies the reflection coefficient,  $\rho_a$  is the soil's apparent resistivity, h shows the finite height of soil top layer, n, represents the total sum of measurements and a, is the distance of the probe in Wenner's test [26,38,44–47]. The effect of the reflection factor (K) on current dispersal into the soil layer has been addressed in [24,40,48–50].

$$\rho_a = \rho_1 \cdot \left\{ 1 + 4 \sum_{n=1}^{\infty} K^n \left[ \frac{1}{\sqrt{1 + \left(\frac{2n \cdot h}{a}\right)^2}} - \frac{1}{\sqrt{4 + \left(\frac{2n \cdot h}{a}\right)^2}} \right] \right\} \quad (1)$$

$$K = \frac{\rho_2 - \rho_1}{\rho_2 + \rho_1} \quad (2)$$

The effect of the upper layer's soil resistivity of a two-layer soil in terms of GPR is explained in [40]. Based on the results presented in [40],  $K < 0$  is denoting that the top layer's soil resistivity is greater than the bottom layer, where the GPR of the grounding grid reduces significantly. That is because the current density is high at the center, and the conductor ends. The fault current discharges directly into the lower resistivity bottom layer. In contrast, there will be a slight reduction in GPR value for  $K > 0$ , in which the top layer's soil resistivity is lower than the bottom layer's resistivity. Since the fault current stays inside the top layer and expands as it disperses into the soil, the density of the current is higher only at the conductor's ends.

Apart from the top soil layer's soil resistivity, the top soil layer's height also affects the grounding performance. Figure 2 displays the grid resistance for 30 m × 30 m with four meshes placed 0.5 m within the soil. The bottom layer resistivity differs to obtain different reflection factors (K), while the top layer's soil resistivity is kept constant. From Figure 2, it can be seen that a homogeneous soil structure exerts no response from the on-grid resistance ( $K = 0$ ). Increasing the depth of the top soil layer for  $K > 0$ , the grid resistance reduces as the top layer's soil depth increases. On the other hand, the grid

resistance increases as the top layer's soil depth increase when  $K < 0$ . The grid resistance values converge with a homogeneous soil structure as the top layer's soil depth approaches infinity [19,50].

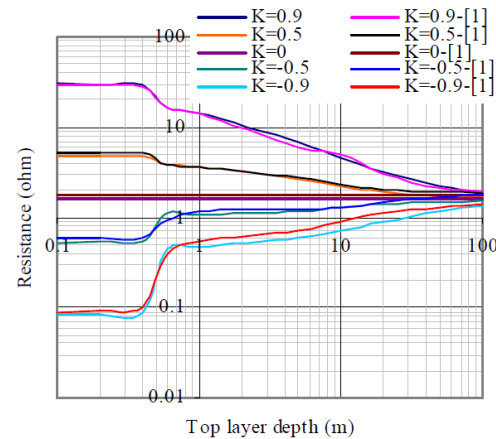


**Figure 2.** Grid resistance of four mesh grounding grids for different top-layer of soil resistivity [50].

When the top layer's soil depth is 0.5 m, which is equivalent to the grid burial depth, a substantial change in grid resistance can be seen. The grounding resistance value is impacted by the bottom layer's soil resistivity when the top layer's is small in height. This is clear that grid resistance is highly affected by properties of bottom layer soil, especially for  $K > 0$ , which can be ignored at high depth, which is two times more of the overall grid diameter. Table 2 summarizes the effect of soil resistivity and depth of the top layers of a two-layer soil on the GPR and grid resistance value.

**Table 2.** The effect of soil resistivity and depth of top layer in a two-layer soil structure.

Soil Resistivity of the Top Layer		Increasing Top Soil Layer Height
$K^1 < 0$	Significant reduction in GPR value	Increases grid resistance
$K^1 > 0$	A slight reduction in GPR value	Reduction in the grid resistance increases
Ref.	[40]	[19,50]

<sup>1</sup>  $K$  is the reflection factor between the first and second soil layers.

### 2.3. Number of Meshes

The number of meshes in a grounding grid can be increased to protect the effectiveness of a grounding system, according to a common understanding of the grounding system. The greater the number of meshes in a grounding grid, the more fault current flows through it and into the soil, decreasing potential gradients above it [39,51].

Unde and Kushare [39] conducted a study on the influence of the number of meshes in a grounding system on the ground resistance,  $R_g$ , in a two-layer soil structure. A  $20\text{ m} \times 20\text{ m}$  grounding grid with 1, 4, 16, and 64 meshes are simulated. A 1000 A current is discharged into the grids and the depth of grid burial is kept at 0.5 m. Case 1 is referring to the top soil layer with lower resistivity than the bottom layer ( $K > 0$ ), while Case 2 is referring to the top soil layer with higher resistivity than the bottom layer ( $K < 0$ ).

Figure 3 below indicates the ground resistance plotted against the number of meshes. The findings show that if the number of meshes for both cases is increased, the ground resistance decreases. However, as the number of meshes increased, the percentage of reduction in grid resistance for the high resistive top layer (case 2) is evident, which is about 41.67% relative compared to the low resistive top layer (case 1), which is just 10.72% (almost constant) as can be seen in Figure 3. This might be owing to the uniform current density dispersion across the grounding conductors in the high resistive top layer and concentrated current density at the grounding perimeter in the low resistive top layer.

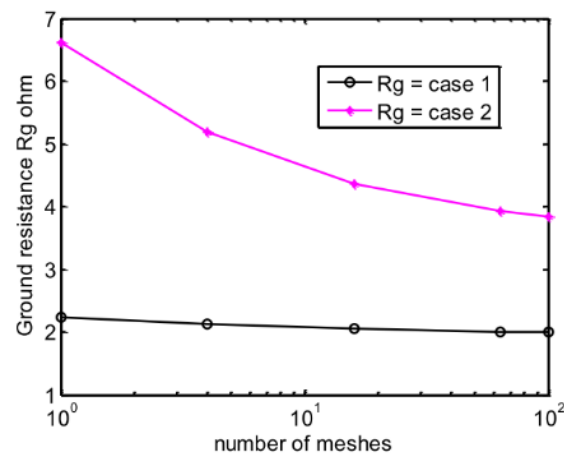


**Figure 3.** Ground resistance,  $R_g$  with a different number of meshes in two-layer soil structure [39].

#### 2.4. Length of Horizontal Conductors

The position for the grounding system installation is determined by the soil layers involved; either uniform soil; horizontal soil, or vertical soil layers. The performance of a grounding system would be influenced by the electrical characteristics of each soil layer present. To demonstrate this, a study was conducted on single short and long horizontal conductors of 10 m and 50 m, respectively, with a 0.005 m radius buried within the top or bottom layer of soil at a depth of 0.75 m [52]. The conductor is energized with a current amplitude of 1 A. The horizontal electrodes are buried at 100  $\Omega\text{m}$  soil layer where it is kept constant as shown in Table 3 and Figure 4 and the relative permittivity of both top and bottom soil layers are also kept constant at 10. The (a) in Table 3 represents the soil layer with high resistivity of 1000  $\Omega\text{m}$  while the (b) represents the soil layer with low resistivity of 10  $\Omega\text{m}$ .

**Table 3.** Parameters of soil layers adapted from [52].

Case	Depth of Upper Layer, $d_1$ (m)	Top Layer Resistivity, $\rho_1$ ( $\Omega\text{m}$ )	Bottom Layer Resistivity, $\rho_2$ ( $\Omega\text{m}$ )
1 (Conductor in a top soil layer)	1.0	100	(a) 1000
			(b) 10
2 (Conductor in a bottom soil layer)	0.5	(a) 1000	100
		(b) 10	

The resistivity of homogeneous soil is assumed as 100  $\Omega\text{m}$  to make a comparison between homogeneous and two-layer soil structures. Table 4 gives the impedance of short and long horizontal grounding conductors, respectively. Although the results presented in [52] consist of various frequencies, only 10 kHz is considered in this paper as it is commonly tested for both lengths of conductors. Both short and long conductors display the same impedance pattern. The impedance of the grounding conductor in Case 1 and Case 2 is higher when the neighbouring soil layer of which the grounding conductor is buried is high (bottom layer-1000  $\Omega\text{m}$ ). In contrast, the impedance is lower when the neighbouring soil layer of which the grounding conductor is buried is low (top layer-100  $\Omega\text{m}$ ) compared to impedance in homogeneous soil [52]. A summary of the grounding impedance in Case 1 and Case 2 is presented in Table 5.

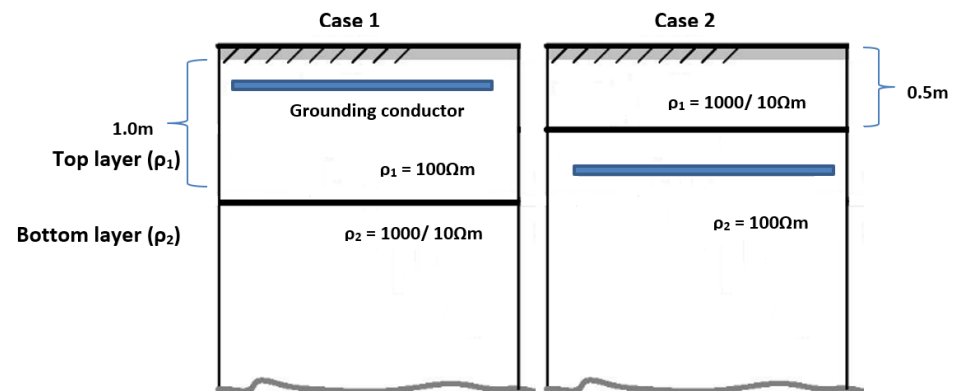


Figure 4. Visual representation of soil layer parameters.

Table 4. The impedance of 10 m and 50 m grounding conductor adapted from [52].

Soil Structure		10 m	50 m
Homogeneous		14.3 $\Omega$	4.4 $\Omega$
Case 1	(a)	35.1 $\Omega$	14.1 $\Omega$
	(b)	8.3 $\Omega$	2.6 $\Omega$
Case 2	(a)	15.6 $\Omega$	4.6 $\Omega$
	(b)	10.8 $\Omega$	3.6 $\Omega$

Table 5. Summary of grounding impedance in Case 1 and Case 2.

	Case 1 (Grounding Conductor in the Top Soil Layer)	Case 2 (Grounding Conductor in the Bottom Soil Layer)
High resistive neighbouring soil (a)	High impedance	Low impedance
Low resistive neighbouring soil (b)	Low impedance	High impedance

Even if the grounding conductor is located in a low resistive soil layer, the impedance is affected by the resistivity of the neighbouring soil layer, according to the findings. Compared to the homogeneous soil layer, the impedance in high resistive neighbouring soil (case 1 and case 2) is higher, while the impedance is lower in low resistive neighbouring soil for both cases. In case 2, the grounding conductor’s impedance is lower than in case 1 when the neighboring soil is highly resistive. This might be because the neighboring soil’s high resistivity (top layer) allows more current to pass to the lower resistivity of the bottom layer, decreasing the grounding impedance. On the other hand, low resistive neighbouring soil (top layer) allows more current flow to the lower resistivity in the top layer, raising grounding impedance. Case 1 exhibits a grounding behavior that is the contrary of case 2.

### 2.5. Length of Vertical Rods

The vertical rod length is a key design element in affecting the grounding behavior and protection in a two-layer soil structure. When it comes to assessing the safety of a grounding system, the placement of vertical rods is crucial [16,53–55]. A study on the effect of the length of vertical rods on a grounding system is conducted in [16]. Two horizontal grounding grids with 150 m  $\times$  150 m and 100 m  $\times$  100 m were analyzed, and four vertical rods were attached to the horizontal grounding grids as in Figure 5. The grids are placed 0.6 m within the soil and the mesh dimension for both grids is 10 m. Figure 5 shows the

comparison between two different grid sizes on grounding resistance in two-layer soil. For two-layer soil, the top layer,  $\rho_1$ , has a resistivity of 200 m while the bottom layer,  $\rho_2$ , has a resistivity of 600 m. The top soil layer is 20-m deep.

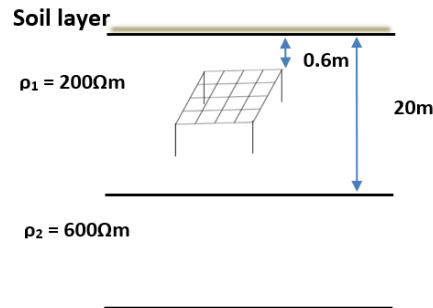


Figure 5. A grounding grid positioning in two-layer soil structure.

It shows that the two curves in Figure 6 are almost superposed, whereas the grounding resistance reduction rate,  $\zeta$  (at the  $y$ -axis) for different grid sizes are almost similar due to the ratio of the corresponding radius and the vertical rod-length ( $L/R_{eq}$ ) (at the  $x$ -axis) is same. Grounding resistance reduction rate,  $\zeta$  measures the grounding resistance reduction when the length of vertical rod varies, which is calculated using Equation (3), while  $R_{eq}$  is the equivalent radius of the horizontal grounding grid calculated using Equation (4) [16].  $S$  represents the horizontal grounding grid area.  $R_0$  denotes the horizontal grounding grid's resistance.  $R_1$  represents the grounding resistance after vertical rods are added [16]. The reduction rate for a larger grounding grid (150 m × 150 m) is lower than the smaller grid (100 m × 100 m) in two-layer soil [16].

$$\zeta = \frac{R_0 - R_1}{R_0} \tag{3}$$

$$R_{eq} = \sqrt{\frac{S}{\pi}} \tag{4}$$

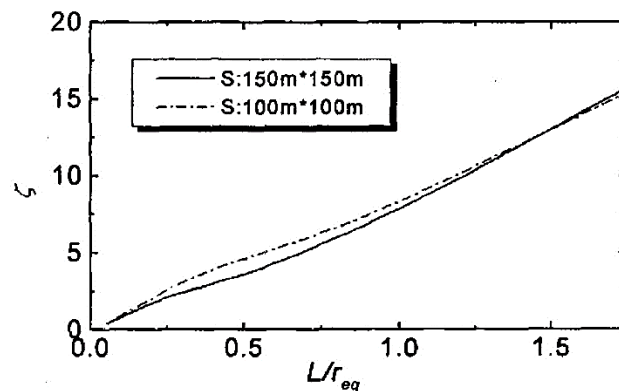


Figure 6. Effect of vertical rod length on decreasing grounding resistance rate in two-layer soil [16].

The findings show that the curves overlap each other when they are far from the two-layer boundary; whereas they diverge significantly when they are near the soil boundary. The resistance reduction rate differs significantly between two different sizes of grounding grids for the same length of vertical rods. The impact of soil resistivity of the top and bottom layers of a two-layer soil structure might explain this phenomenon. According to research findings in [11,55–57], when the length of the rod is long enough to penetrate the high resistive bottom soil layer, its resistivity impacts the behavior of the grounding system, increasing grid resistance. The length of rods to be installed at the grounding grid

is dependent on the resistivity of the soil layer. Longer rods are only effective in two-layer soil with lower resistivity at the bottom since more current will spread via a longer rod, making the grounding system safe. For a low resistive top layer, shorter rods are sufficient.

### 3. Effect of Horizontal Three-Layer Soil Characteristics on Grounding System Performances

#### 3.1. Apparent Soil Resistivity and Reflection Factor ( $K$ )

Grounding performance analysis in horizontal three-layer soil structure is not as common as horizontal two-layer soil structure due to its complexity in computation. Since the computations and analysis of grounding systems which deal with the multilayer, soil structure are usually complex; the equations and the derivations of three-layered soils' apparent soil resistivity were explained in [49,58,59], and are discussed in this section. Figure 7a,b below represent the three-layer soil structure.

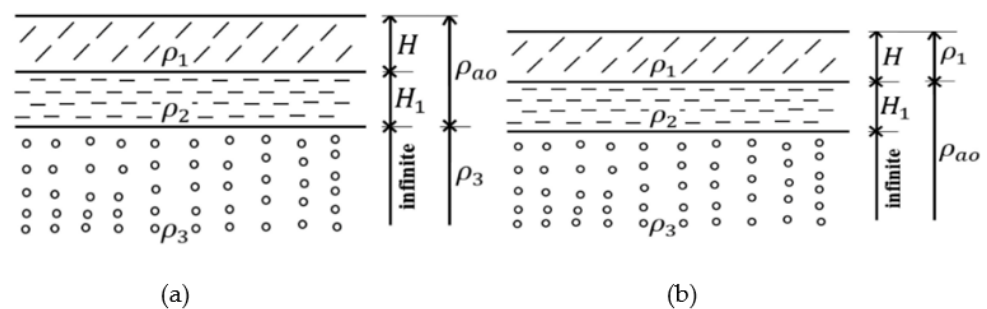


**Figure 7.** Horizontal three-layer soil structure (a) The first and second layers are represented as  $\rho_{a0}$ , (b) The second and third layers are represented as  $\rho_{a0}$  [50].

According to IEEE 80 [42], the initial apparent soil resistivity between the first and second layers is calculated using Equations (5) and (6) and is represented by  $\rho_{12}$  where  $\rho_1$  and  $\rho_2$  are the resistivities of the first and second layers, respectively, and  $H'$  is the thickness of the first layer, as shown in Figure 7a. The apparent soil resistivity of the three layers is then calculated using the following IEEE 80 equation, with the first- and second layers having soil resistivity of  $\rho_{12}$  as one layer and the third layer resistivities having a resistivity of  $\rho_3$  as another layer. In this example,  $K'$  is the reflection factor defined in Equation (7).

$$\rho_{12} = \frac{l_2(\rho_1\rho_2)}{(\rho_2(H' - h) + \rho_1(l_2 + h - H'))} \tag{5}$$

$$\rho_a = \frac{l_2(\rho_{12}\rho_3)}{(\rho_3(H' - h) + \rho_{12}(l_2 + h - H'))} \tag{6}$$

$$K' = \frac{\rho_3 - \rho_{12}}{\rho_3 + \rho_{12}} \tag{7}$$

Figure 7b depicts the calculations in Equations (8)–(10) and is presented according to IEEE 80 [42]. The apparent soil resistivity of the second and third layers is  $\rho_{23}$ ; the resistivity values of the second and third soil layers are  $\rho_2$  and  $\rho_3$ , respectively. As illustrated in Figure 7b,  $H$  stands for the height of first layer soil,  $H_1$  for the second layer's height,  $l_2$  for the length of grounding rods, and  $h$  for the grounding laying depth. The reflection factor,  $K''$  is defined in Equation (10).

$$\rho_{23} = \frac{l_2(\rho_2\rho_3)}{(\rho_3(H_1 - h) + \rho_2(l_2 + h - H_1))} \tag{8}$$

$$\rho_a = \frac{l_2(\rho_1\rho_{23})}{(\rho_{23}(H - h) + \rho_1(l_2 + h - H))} \tag{9}$$

$$K'' = \frac{\rho_{23} - \rho_1}{\rho_{23} + \rho_1} \tag{10}$$

The performance of the grounding grid is investigated using two three-layered soil structures with different soil resistivities and reflection factors, as shown in Table 6. The apparent resistivity of the soil is calculated using Equations (5)–(10).

**Table 6.** Soil data for two different structures adapted from [50].

Structure	Soil Layer	Resistivity (Ωm)	Soil Thickness (m)
A	1	200	2
	2	20–2000	2
	3	300	∞
B	1	200	2
	2	1000	2
	3	20–2000	∞

Figure 8a indicates that a rise in the positive reflection factors (+K) reduces the apparent soil resistivity when  $\rho_{12} > \rho_3$  and increases the apparent soil resistivity when  $\rho_3 > \rho_{12}$  for negative reflection factors (−K) in structure A. The same Figure 8a also indicates that a vice versa trend of the apparent soil resistivity in case of  $\rho_1 > \rho_{23}$  or  $\rho_3 > \rho_{12}$ . Similar measurements are conducted using structure (B), where the apparent soil resistivity increases with positive reflection factor in both cases of ( $\rho_{23} > \rho_1$ ) and ( $\rho_3 > \rho_{12}$ ) and reduces for negative reflection factors when ( $\rho_{12} > \rho_3$  or when  $\rho_1 > \rho_{23}$ ) given in Figure 8b [49]. A similar pattern on apparent resistivity behavior can also be seen in [58].

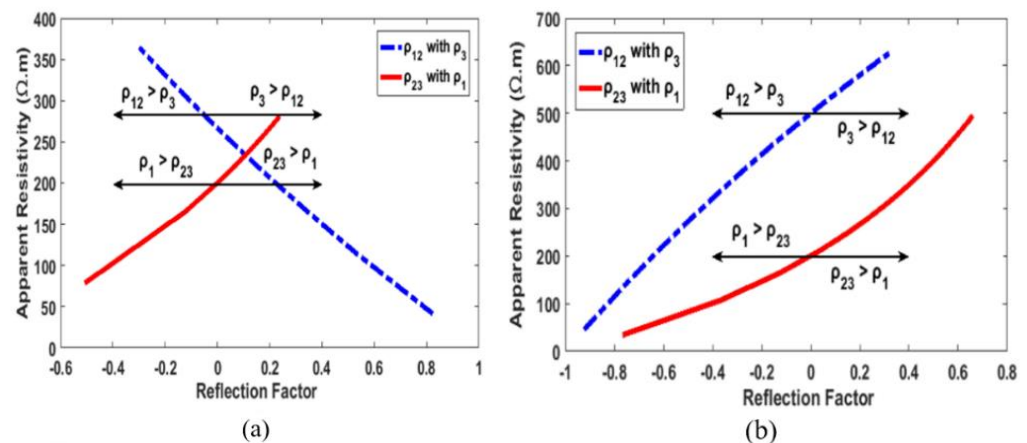


**Figure 8.** The relationship between the soil’s apparent resistivity and the reflection factor (K) (a) soil structure (A) (b) soil structure (B) [49].

As previously stated, analyzing the performance of a grounding system in a horizontal three-layer soil structure is more complex and difficult than in a two-layer soil structure. There is no comprehensive and extensive study on the performance of grounding systems in horizontal three-layer soil constructions. In next Sections 3.2 and 3.3, a few relevant works on the influence of grounding design parameters, such as grounding electrode types and vertical rod length in horizontal three-layer soil structures will be discussed.

### 3.2. Types of Grounding Electrodes

The analysis in [60] was conducted for three types of grounding electrodes namely; liner, ring-shaped and cross-shaped. The placement of ring-shaped grounding electrodes and directions for X and Y coordinates of the three-layer soil are shown in Figure 9. The same placement is applicable for the linear grounding electrode. The electrodes are buried

0.05 m depth into the soil. Only the linear and ring-shaped grounding electrodes will be discussed in this section to summarize the information on the effect of different types of grounding electrodes on grounding performance in horizontal three-layer soil, as the ring-shaped grounding electrode has the best dispersion properties and the linear grounding electrode has the poorest. Table 7 shows the maximum current and potential distribution for linear and ring-shaped grounding electrodes.

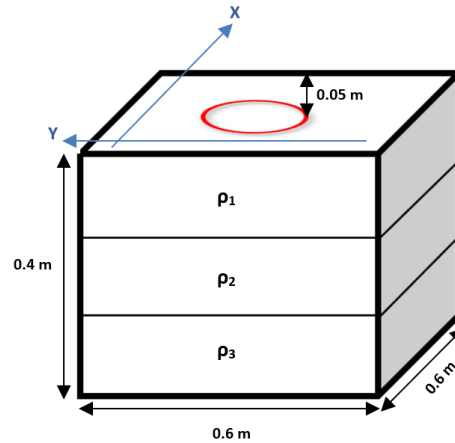


Figure 9. Placement of ring-shaped grounding electrodes in three-layer soil structure with X and Y coordinates.

Table 7. Current and potential distribution for linear and ring-shaped grounding electrodes.

	Linear	Ring-Shaped
Peak Current density (A/m <sup>2</sup> )	67.4	43
Optimum Potential (V)	278	173

For linear grounding electrodes in Figure 10a,b, the peak current density is likely to be right above the linear grounding electrode’s edges. The current peak value of 65.9 A/m<sup>2</sup> occurs at 0.25 m and 0.35 m of Y coordinates. The current density decreases to 25 A/m<sup>2</sup> at the soil structure boundary. The optimum potential can be seen right above the middle of the linear grounding electrode [60].

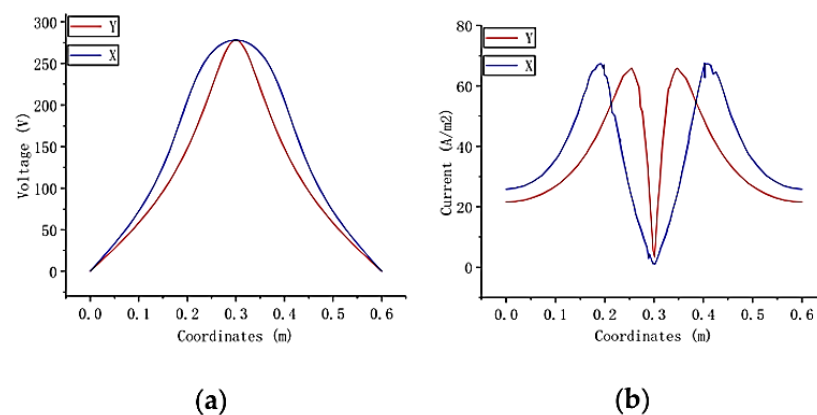
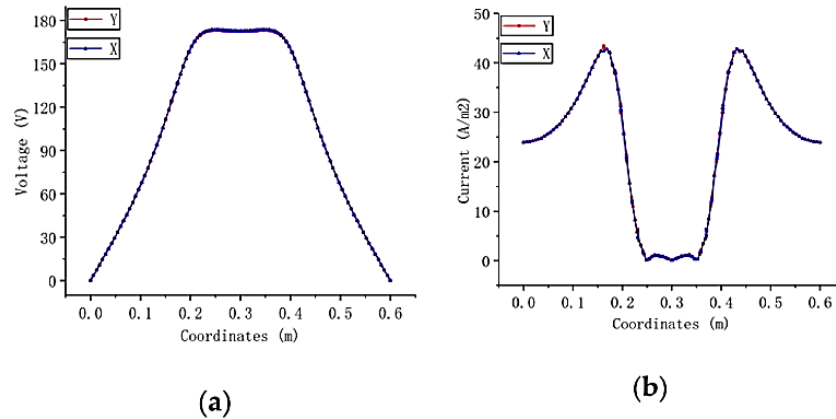


Figure 10. Current density and potential distribution curves for X and Y directions of linear grounding electrode (a) potential distribution (b) current density distribution [60].

The peak current density can be seen at about 0.15 m from the center point in a circular field for the ring-shaped grounding electrode as in Figure 11a,b. The surface current density is near to 0 in a circular field about 0.05 m from the core and two smaller current

peaks of  $1 \text{ A/m}^2$ . The current density dropped to  $24 \text{ A/m}^2$  at the soil's border. On the other hand, the optimum potential can be seen right above the ring-shaped grounding electrode structure.



**Figure 11.** Current density and potential distribution graphs for the X and Y directions of the ring-shaped grounding electrode. (a) Potential distribution (b) current density distribution [60].

In both X and Y directions, it can be deduced that the current density and potential distribution curves for ring-shaped grounding electrodes overlap. Since both types of grounding electrodes are fully symmetrical, this overlap makes sense. Furthermore, under the same conditions, the current and voltage in the soil surrounding the ring-shaped grounding electrode are 35–40% [60] lower than those around the linear grounding electrode.

### 3.3. Vertical Grounding Rods

Similar to horizontal two-layer soil, the length of vertical rods connected to a grounding grid plays a vital part in defining grounding behavior and protection. The effect of vertical grounding rod length in a horizontal three-layer soil configuration is studied in Ref [16]. The effect of vertical grounding rods on the decrease rate of grounding resistance is seen in Figure 12. High resistivity layer (H) of  $1000 \Omega\text{m}$ , medium resistivity layer (M) of  $500 \Omega\text{m}$  and low resistivity layer (L) of  $100 \Omega\text{m}$  comprise a three-layer soil structure. The first soil layer is 10-m deep, while the second soil layer is 50-m deep. The graph in Figure 12 shows the grounding resistance reduction rate,  $\zeta$  at the y-axis, and the ratio of the corresponding radius and the vertical rod-length ( $L/R_{eq}$ ) at the x-axis, where  $R_{eq}$  is the equivalent radius of the horizontal grounding grid calculated using Equation (4) from Section 2.5.

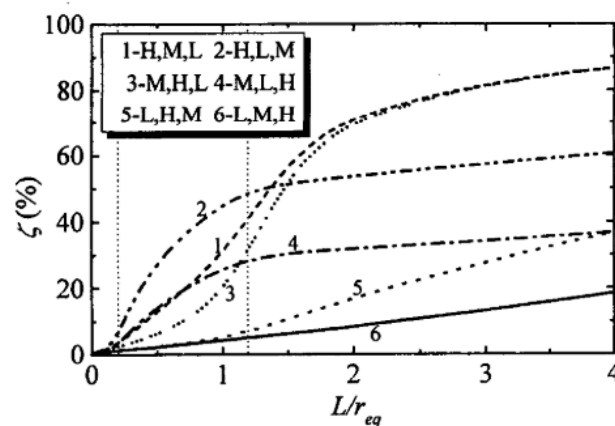


**Figure 12.** The effect of additional vertical rods on the decreasing rate of grounding resistance [16].

From the graph, it can be seen that a similar behavioural pattern is present in horizontal two-layer soil structures. The findings show that long rods will not be able to reduce the grounding resistance when the first layer soil resistivity is low, as can be seen at 'L, H, M' (5) and 'L, M, H' (6). It is also found that the grounding resistance reduction rate of the 'M, L, H' (4) is lower than that of 'M, H, L' (3) before the vertical rods reach the bottom layer. This is attributed to the effect of the second soil layer of low resistivity. The low resistivity second layer causes more current to disperse thus the reduction rate of grounding resistance is lower compared to the 'M, H, L' soil structure. Therefore, based on the results, it is recommended that it is best for vertical rods to remain in the second soil layer in 'M, L, H' soil structure, compared to the 'M, H, L', soil structure where the vertical rods need to long enough to enter the bottom layer.

#### 4. Effect of Vertical Two-Layer Soil Characteristics on Grounding System Performances

*Electrodes Spacing (a), the Distance between Electrodes and Two-Layers Interface (d) and Electrodes Angle ( $\beta$ ) on Apparent Resistivity ( $\rho_a$ )*

Commonly, before measuring the actual soil parameters, horizontal soil layers, either two-layers soil or several soil layers are recommended. For representing more realistic scenarios, vertical-layer soil may be considered. This will assist in clarifying the features of soil properties and their measurements [48,61–69]. Otherwise, in calculating the soil parameters and grounding system designs, the error in assuming soil structure would probably result in a malfunction. The calculation and analysis of vertical two-layer soil structures are more complex than horizontal two-layer soil structures. As a result, a comprehensive and extensive analysis of grounding performance in vertical two-layer soil structures has yet to be performed.

The general apparent resistivity expression  $\rho_a$ , in vertical-layered soil, as in Equation (11) is suggested in [48] to determine the relationship between the locations of 4 electrodes in Wenner's method and the apparent resistivity. According to Equation (11), "a" is the distance between the four electrodes (m),  $\rho_1$  is the resistivity of the first soil layer ( $\Omega\text{m}$ ), k is the reflection factor between first and second soil layers, "d" represents the standard distance between the first electrode and the border between the first and second soil layer and the angle between a perpendicular line to the soil border and the line where four electrodes are positioned is represented by angle,  $\beta$ . The parameters of vertical soil structure are shown in Figure 13.

$$\rho_a = a\rho_1 \left( \frac{1}{a} + \frac{k}{\sqrt{4d^2 + 4da \cos \beta + a^2}} + \frac{k}{\sqrt{4(d+3a \cos \beta)(d+2a \cos \beta) + a^2}} - \frac{k}{\sqrt{4d^2 + 8da \cos \beta + 4a^2}} - \frac{k}{\sqrt{4(d+3a \cos \beta)(d+a \cos \beta) + 4a^2}} \right) \quad (11)$$

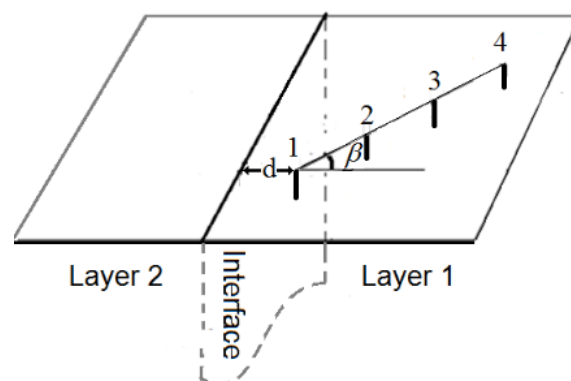


Figure 13. Vertical two-layer soil structure [48,67].

There are two cases (Case 1 and Case 2) that were analyzed based on the apparent soil resistivity using Equation (11) in [67]. The analysis was conducted to examine the effects of varying electrode spacing 'a', and the distance from two-layer soil interface 'd' and the

angle ' $\beta$ ' between a perpendicular line to the soil border and the line where four electrodes are positioned on the apparent resistivity. The results are summarized in Table 8.

**Table 8.** Summary of performance of apparent resistivity with varying parameters ' $a$ ', ' $d$ ' and  $\beta$ .

	Case 1 ( $\rho_1=100 \Omega\text{m}$ ), ( $\rho_2=1000 \Omega\text{m}$ )	Case 2 ( $\rho_1=1000 \Omega\text{m}$ ), ( $\rho_2=100 \Omega\text{m}$ )
Distance, ' $a$ ' between electrodes increases	Apparent resistivity started to increase significantly until a certain distance, and then increases with a small rate	Apparent resistivity started to decrease significantly until a certain distance, and then decreases with a small rate
The distance, ' $d$ ' increases	Due to the impact of the second layer with high resistivity, the apparent resistivity reduces.	Due to the impact of the second layer with low resistivity, the apparent resistivity increases.
The angle, $\beta$ increases.	The apparent resistivity increases	The apparent resistivity decreases

$\rho_1$  is the resistivity of the first soil layer either on the left or right of the vertical soil boundary ( $\Omega\text{m}$ ).  $\rho_2$  is the resistivity of the second soil layer neighbouring the first soil layer ( $\Omega\text{m}$ ).

Zeng et al. [62] reported important research on the position of the current electrode on the grounding system in vertically layered soil where the grounding resistance is determined by the 0.618 DCG procedure for grounding resistance calculation in the analysis. In the analysis, the DCG technique refers to the distance between the test current electrode and the grounding system. The fall-of-potential approach was used to examine the apparent grounding resistance curves in various measurement routes. The investigation found that if the measuring lead is positioned parallel to the vertical soil border, which is within the engineering range, the measurement error of the 0.618 techniques is extremely minimal. Even if the distance between the grounding system and the potential electrode is longer, the findings in [62] concluded that positioning the potential electrode on the opposite side of the current electrode in all measurement paths is not recommended because it leads to a measurement error of more than 10%.

## 5. Conclusions

The existing standards available to design a grounding system are typically relevant only for homogeneous soil conditions, as opposed to the fact that most of the soil structures on this earth are non-homogenous. The layered structure of a non-homogeneous soil can affect the ground resistance and ground potentials on soil profile particularly when the soil resistivity between layers differs enormously. However, owing to the complexities of computations needed to resolve the problem, often the soils are assumed to be homogenous, which resulted in significant inaccuracies. In varying soil conditions, the performance of different grounding grid parameters may dramatically change. Although an exact comparison is impossible because grounding grid designs vary depending on the location to be installed, a broad overview of grounding performance as design changes and their effects as soil layers and their corresponding characteristics change will be useful in providing more information on safe grounding designs in non-homogeneous soil.

The design parameters for grounding behavior analysis in a horizontal two-layer soil structure were varied in terms of grid depth, mesh number, and length of horizontal conductors and vertical rods, while the soil characteristics were altered in terms of depth and resistivity of the first soil layer. It can be observed that the resistivity of each soil layer has an impact on grounding behavior and safety. For example, the GPR reduces when the depth of the grid increases until it reaches the border of the top layer and increases after the grid enters the bottom layer with high resistivity when the soil resistivity in the bottom layer  $\rho_2$  is higher than the top soil layer  $\rho_1$ . Longer vertical rods in a horizontal two-layer soil structure are only effective when the bottom layer's soil resistivity,  $\rho_2$  is lower than the top soil layer's resistivity,  $\rho_1$ . When the soil resistivity in the bottom layer  $\rho_2$  is higher than the top soil layer  $\rho_1$  increasing the top soil layer's depth and resistivity for simulation purposes increases the GPR and grid resistance, while vice versa shows

a substantial reduction. This demonstrates the impact of the first soil layer's depth and corresponding resistivity on grounding behavior.

The design parameters for grounding behavior analysis in a horizontal three-layer soil structure were changed in terms of grounding electrode types and vertical rod lengths. The analysis utilized ring-shaped and linear grounding electrodes in a three-layer horizontal soil structure and found that the ring-shaped grounding electrode has the best current and potential dispersion properties, while the linear grounding electrode has the poorest. The findings for the length of vertical rods are similar to the horizontal two-layer soil structure when it reaches the low resistive soil layer. Besides, the study on the impact of reflection factor,  $K$ , on the soil apparent resistivity shows that when the soil resistivity in the bottom layer is higher than the top layer ( $K > 0$ ), the apparent resistivity reduces for  $\rho_{12} < \rho_2$  and increases for  $\rho_{23} < \rho_1$  and vice versa for ( $K < 0$ ).

Vertical two-layer soil structures are more difficult to compute and analyze than horizontal two-layer soil structures. As a result, a comprehensive study of grounding performance in vertical two-layer soil structures has yet to be performed. The only analysis in vertical soil layer was conducted to examine the effects of varying electrode spacing 'a', and the distance from two-layer soil interface 'd' and the angle ' $\beta$ ' between a perpendicular line to the soil border and the line where four electrodes are positioned on the apparent resistivity. The analysis concluded that the apparent resistivity increases as the distance 'a' and the angle ' $\beta$ ' increases while the that the apparent resistivity reduces as the distance 'd' increases.

Relatively few detailed studies have been published on the influence of multilayer soil, particularly on the effect of the grounding-grid design parameters in vertical soil structure. Therefore, further works on the effect of multilayer soil layers and vertical soil layers on grounding system performances with various design parameters such as the grounding grid dimensions, number, and position of vertical electrodes attached to the main grounding grid, need to be conducted. The outcomes of these analyses could serve as an important guide on the substation grounding grid design to be appropriate and safer for the public and personnel.

**Author Contributions:** N.P., writing—original draft preparation; M.O., writing—review and editing; A.M.A., supervision; M.Z.A.A.K., supervision. All authors have read and agreed to the published version of the manuscript.

**Funding:** This research was funded by the Ministry of Higher Education (MOHE) Malaysia through the Fundamental Research Grant Scheme (FRGS) 2020 under Grant FRGS/1/2020/TK0/UNITEN/02/13.

**Institutional Review Board Statement:** Not applicable.

**Informed Consent Statement:** Not applicable.

**Data Availability Statement:** Not applicable.

**Acknowledgments:** The authors would like to thank the Ministry of Higher Education (MOHE) Malaysia through Fundamental Research Grant Scheme (FRGS) 2020 under FRGS/1/2020/TK0/UNITEN/02/13 and BOLD Publication Fund.

**Conflicts of Interest:** The authors declare no conflict of interest.

## References

1. Kižlo, M.; Kanbergs, A. The Causes of the Parameters Changes of Soil Resistivity. *Power Electr. Eng.* **2010**, *25*, 43–46. [[CrossRef](#)]
2. Sing, L.K.; Yahaya, N.; Othman, S.R.; Fariza, S.N.; Noor, N.M. The Relationship between Soil Resistivity and Corrosion Growth in Tropical Region. *J. Corros. Sci. Eng.* **2013**, *16*, 1–11.
3. CIGRE 781. *Impact of Soil-Parameters Frequency Dependence on the Response of Grounding Electrodes and on the Lightning Performance of Electrical Systems*; e-cigre.org: Paris, France, 2019.
4. Lee, C.H.; Chang, C.N.; Jiang, J.A. Evaluation of Ground Potential Rises in a Commercial Building during a Direct Lightning Stroke Using CDEGS. *IEEE Trans. Ind. Appl.* **2015**, *51*, 4882–4888. [[CrossRef](#)]
5. Martins-Britto, A.G.; Lopes, F.V.; Rondineau, S.R.M.J. Multilayer Earth Structure Approximation by a Homogeneous Conductivity Soil for Ground Return Impedance Calculations. *IEEE Trans. Power Deliv.* **2020**, *35*, 881–891. [[CrossRef](#)]

6. Zheng, D.; Li, X.; Zhao, T.; Wen, J.; Van Der Velde, R.; Schwank, M.; Wang, X.; Wang, Z.; Su, Z. Impact of Soil Permittivity and Temperature Profile on L-Band Microwave Emission of Frozen Soil. *IEEE Trans. Geosci. Remote Sens.* **2020**, *59*, 1–14. [[CrossRef](#)]
7. Mokhtari, M.; Abdul-Malek, Z.; Salam, Z. The Effect of Soil Ionization on Transient Grounding Electrode Resistance in Non-Homogeneous Soil Conditions. *Int. Trans. Electr. Energy Syst.* **2016**, *26*, 1462–1475. [[CrossRef](#)]
8. He, J.; Zeng, R.; Zhang, B. *Methodology and Technology for Power System Grounding*; John Wiley & Sons Singapore Pte. Ltd.: Singapore, 2013; ISBN 9781118254950.
9. Ametani, A.; Nagaoka, N.; Baba, Y.; Teruo Ohno, K.Y. *Power System Transients: Theory & Application*, 2nd ed.; CRC Press: Boca Raton, FL, USA, 2017; ISBN 9781498782371.
10. Warne, A.H.D. *Advances in High Voltage Engineering*; The Institution of Engineering and Technology: Stevenage, UK, 2007; ISBN 9780852961582.
11. Batista, R.; Paulino, J.O.S. A Practical Approach to Estimate Grounding Impedance of a Vertical Rod in a Two-Layer Soil. *Electr. Power Syst. Res.* **2019**, *177*, 105973. [[CrossRef](#)]
12. Jesenik, M.; Trlep, M. Testing of Multi Layered Soil Models Based on Data Obtained from Finite Element Models with Known Soil Structures Using Metaheuristics for Parameters' Determination. *Appl. Soft Comput. J.* **2020**, *95*, 106541. [[CrossRef](#)]
13. de Araújo, A.R.J.; Colqui, J.S.L.; de Seixas, C.M.; Kurokawa, S.; Salarieh, B.; Pissolato Filho, J.; Kordi, B. Computation of Ground Potential Rise and Grounding Impedance of Simple Arrangement of Electrodes Buried in Frequency-Dependent Stratified Soil. *Electr. Power Syst. Res.* **2021**, *198*, 107364. [[CrossRef](#)]
14. Dan, Y.; Zhang, Z.; Zhao, H.; Li, Y.; Ye, H.; Deng, J. A Novel Segmented Sampling Numerical Calculation Method for Grounding Parameters in Horizontally Multilayered Soil. *Int. J. Electr. Power Energy Syst.* **2021**, *126*, 106586. [[CrossRef](#)]
15. Anggoro, B.; Dharmawanwas, R.H.; Ningrum, H.N.K.; Burhan, J.; Bin Tamjis, M.R. Grounding Impedance Characteristics for Two-Layer Soil of Vertical Rod Configuration with Variation of Length and Diameter. *Int. J. Electr. Eng. Inform.* **2018**, *10*, 799–815. [[CrossRef](#)]
16. Zeng, R.; He, J.; Wang, Z.; Gao, Y.; Sun, W.; Su, Q. Analysis on Influence of Long Vertical Grounding Electrodes on Grounding System for Substation. In Proceedings of the PowerCon 2000. 2000 International Conference on Power System Technology. Proceedings (Cat. No.00EX409), Perth, Australia, 4–7 December 2000; pp. 1475–1480. [[CrossRef](#)]
17. Ilievska, R. Earth Resistance and Calculation of Earthing. *Distrib. Ind. Syst.* **2017**, *1*, 4–27.
18. Nikolovski, S.; Knežević, G.; Baus, Z. Assessment of Step and Touch Voltages for Different Multilayer Soil Models of Complex Grounding Grid. *Int. J. Electr. Comput. Eng.* **2016**, *6*, 1441–1455. [[CrossRef](#)]
19. Nahman, J.; Paunovic, I. Resistance to Earth of Earthing Grids Buried in Multi-Layer Soil. *Electr. Eng.* **2006**, *88*, 281–287. [[CrossRef](#)]
20. Lu, T.; Qi, L.; Cui, X. Effect of Multilayer Soil on the Switching Transient in Substations. *IEEE Trans. Magn.* **2006**, *42*, 843–846. [[CrossRef](#)]
21. Sekki, D.; Nekhoul, B.; Kerroum, K.; El Khamlichi Drissi, K.; Poljak, D. Transient Behaviour of Grounding System in a Two-Layer Soil Using the Transmission Line Theory. *Automatika* **2014**, *55*, 306–316. [[CrossRef](#)]
22. Nahman, J.; Djordjevic, V. Resistance to Earth of Substation Earth Electrodes in Uniform and Two-Layer Soils. *Electr. Eng.* **1997**, *80*, 337–342. [[CrossRef](#)]
23. Stanisic, S.; Radakovic, Z. Calculation of Touch Voltage Based on Physical Distribution of Earth Fault Current. *IEEE Trans. Power Deliv.* **2017**, *32*, 2246–2254. [[CrossRef](#)]
24. Nassereddine, M.; Rizk, J.; Nagrial, M.; Hellang, A. Estimation of Apparent Soil Resistivity for Two-Layer Soil Structure. *Int. J. Energy Environ.* **2010**, *1*, 427–446.
25. Vycital, V.; Topolaneck, D.; Toman, P.; Ptacek, M. Sensitivity Analysis of Earthing System Impedance for Single and Multilayered Soil. *CIGRE Open Access Proc. J.* **2017**, *2017*, 428–431. [[CrossRef](#)]
26. Nassereddine, M.; Rizk, J.; Nasserddine, G. Soil Resistivity Data Computations; Single and Two-Layer Soil Resistivity Structure and Its Implication on Earthing Design. *Int. J. Electr. Comput. Eng.* **2013**, *7*, 35–40.
27. Yang, J.; Zou, J. Parameter Estimation of a Horizontally Multilayered Soil with a Fast Evaluation of the Apparent Resistivity and Its Derivatives. *IEEE Access* **2020**, *8*, 52652–52662. [[CrossRef](#)]
28. Ma, J.; Dawalibi, F.P. Computerized Analysis of Grounding Plates in Multilayer Soils. *IEEE Trans. Power Deliv.* **2009**, *24*, 650–655. [[CrossRef](#)]
29. Coelho, R.R.A.; Pereira, A.E.C.; Neto, L.M. A High-Performance Multilayer Earth Parameter Estimation Rooted in Chebyshev Polynomials. *IEEE Trans. Power Deliv.* **2018**, *33*, 1054–1061. [[CrossRef](#)]
30. Li, Z.X.; Rao, S.W. The Inversion of One-Dimensional Soil Parameters in the Frequency Domain with Considering Multilayered Earth Based on Simulated Annealing Algorithm. *IEEE Trans. Electromagn. Compat.* **2020**, *62*, 425–432. [[CrossRef](#)]
31. Zhao, H.; Fortin, S.; Dawalibi, F.P. Analysis of Grounding Systems Including Freely Oriented Plates of Arbitrary Shape in Multilayer Soils. *IEEE Trans. Ind. Appl.* **2015**, *51*, 5189–5197. [[CrossRef](#)]
32. Gonos, I.F.; Stathopoulos, I.A. Estimation of Multilayer Soil Parameters Using Genetic Algorithms. *IEEE Trans. Power Deliv.* **2005**, *20*, 100–106. [[CrossRef](#)]
33. Pereira, W.R.; Soares, M.G.; Neto, L.M. Horizontal Multilayer Soil Parameter Estimation Through Differential Evolution. *IEEE Trans. Power Deliv.* **2016**, *31*, 622–629. [[CrossRef](#)]
34. Calixto, W.P.; Neto, L.M.; Wu, M.; Yamanaka, K.; Da Paz Moreira, E. Parameters Estimation of a Horizontal Multilayer Soil Using Genetic Algorithm. *IEEE Trans. Power Deliv.* **2010**, *25*, 1250–1257. [[CrossRef](#)]

35. Permal, N.; Osman, M.; Kadir, M.Z.A.A.; Ariffin, A.M. Review of Substation Grounding System Behavior Under High Frequency and Transient Faults in Uniform Soil. *IEEE Access* **2020**, *8*, 142468–142482. [[CrossRef](#)]
36. Abdel-Salam, M.; Ahmed, A.; Nayel, M.; Zidan, A. Surface Potential and Resistance of Grounding Grid Systems in Homogeneous Soil. *Electr. Power Compon. Syst.* **2007**, *35*, 1093–1109. [[CrossRef](#)]
37. Kumar, M.; Singh, G. Design of Grounding System for an Electrical Substation: An Overview. *Int. J. Sci. Eng. Res.* **2014**, *5*, 246–248.
38. Vyas, K.A.; Jamnani, J.G. Optimal Design of Grounding System for HV/EHV Substations in Two Layered Soil. *Int. J. Emerg. Technol. Adv. Eng.* **2012**, *2*.
39. Unde, M.G.; Kushare, B.E. Grounding Performance of Substation in Two Layer Soil- A Parametric Analysis. *Int. J. Eng. Sci. Emerg. Technol.* **2012**, *1*, 69–76. [[CrossRef](#)]
40. Puttarach, A.; Chakpitak, N.; Kasirawat, T.; Pongsriwat, C. Substation Grounding Grid Analysis with the Variation of Soil Layer Depth Method. In Proceedings of the 2007 IEEE Lausanne Power Tech, Lausanne, Switzerland, 1–5 July 2007; pp. 1881–1886. [[CrossRef](#)]
41. Moreno, J.; Simon, P.; Faleiro, E.; Asensio, G.; Fernandez, J.A. Estimation of an Upper Bound to the Value of the Step Potentials in Two-Layered Soils from Grounding Resistance Measurements. *Materials* **2020**, *13*, 290. [[CrossRef](#)]
42. IEEE. *IEEE Guide for Safety in AC Substation Grounding*; IEEE Std 80-2013; IEEE: Piscataway, NJ, USA, 2013; Volume 2000, ISBN 0738119261.
43. IEEE. *IEEE Guide for Measuring Earth Resistivity, Ground Impedance, and Earth Surface Potentials of a Grounding System*; IEEE Std 81-2012; IEEE: Piscataway, NJ, USA, 2012; Volume 2012, ISBN 978-0-7381-8028-1.
44. Rajab Investigations of Two-Layer Earth Parameters at Low Voltage: Measurements and Calculations. *Am. J. Eng. Appl. Sci.* **2009**, *2*, 165–170. [[CrossRef](#)]
45. Ayodele, T.R.; Ogunjuyigbe, A.S.O.; Oyewole, O.E. Comparative Assessment of the Effect of Earthing Grid Configurations on the Earthing System Using IEEE and Finite Element Methods. *Eng. Sci. Technol. Int. J.* **2018**, *21*, 970–983. [[CrossRef](#)]
46. Gursu, B.; Cevdet, M. Limiting GPR in a Two-Layer Soil Model via Genetic Algorithms Limiting GPR in a Two-Layer Soil Model via Genetic Algorithms. *J. Frankl. Inst.* **2019**, *346*, 768–783. [[CrossRef](#)]
47. Salaraa, M.M.; El Sherbiny, M.M.; Chow, Y.L. A Formula for Resistance of Substation Grounding Grid in Two-Layer Soil. *IEEE Trans. Power Deliv.* **1995**, *10*, 1255–1262. [[CrossRef](#)]
48. Nayel, M. Study Apparent Grounding Resistivity in Vertical-Layer Soil. *Electr. Power Compon. Syst.* **2014**, *42*, 845–851. [[CrossRef](#)]
49. Gouda, O.E.; El-Saied, T.; Salem, W.A.A.; Khater, A.M.A. Evaluations of the Apparent Soil Resistivity and the Reflection Factor Effects on the Grounding Grid Performance in Three-Layer Soils. *IET Sci. Meas. Technol.* **2019**, *13*, 469–477. [[CrossRef](#)]
50. Zaini, H.G.; Ghoneim, S.S. Earth Surface Potential and Grounding Resistance for Grounding Grid in Two-Layer Model Soil. In Proceedings of the 2012 IEEE International Conference on Power System Technology (POWERCON), Auckland, New Zealand, 30 October–2 November 2012. [[CrossRef](#)]
51. Nahman, J.; Paunovic, I. Mesh Voltages at Earthing Grids Buried in Multi-Layer Soil. *Electr. Power Syst. Res.* **2010**, *80*, 556–561. [[CrossRef](#)]
52. Arnautovski-Toseva, V.; Grcev, L.; El Khamlichi Drissi, K. High Frequency Electromagnetic Analysis of Horizontal Grounding Conductor and Near-by Passive Parallel Conductor within Two-Layer Soil. In Proceedings of the 2007 15th International Conference on Software, Telecommunications and Computer Networks, Split, Croatia, 27–29 September 2007; pp. 111–115. [[CrossRef](#)]
53. Myint, S.; Aung Oo, Y. Performance Analysis of Actual Step and Mesh Voltage of Substation Grounding System with the Variation of Length and Number of Ground Rod. *Int. J. Sci. Eng. Appl.* **2014**, *3*, 10–17. [[CrossRef](#)]
54. Chen, L.H.; Chen, J.F.; Liang, T.J.; Wang, W.I. Calculation of Ground Resistance and Step Voltage for Buried Ground Rod with Insulation Lead. *Electr. Power Syst. Res.* **2008**, *78*, 995–1007. [[CrossRef](#)]
55. Araujo, A.R.J.; Colqui, J.S.L.; Kurokawa, S.; Pissolato, J. A New Approach to Compute Grounding Impedance of Rods in a Frequency Dependent Multi-Layer Soil. In Proceedings of the 2020 IEEE Power & Energy Society General Meeting (PESGM), Montreal, QC, Canada, 2–6 August 2020; pp. 27–31. [[CrossRef](#)]
56. Buba, S.D.; Wan Ahmad, W.F.; Ab Kadir, M.Z.A.A.; Gomes, C.; Jasni, J.; Osman, M. Reduction of Earth Grid Resistance by Addition of Earth Rods to Various Grid Configurations. *ARPJ. Eng. Appl. Sci.* **2016**, *11*, 4533–4538.
57. Permal, N.; Osman, M.; Ariffin, A.M.; Ab Kadir, M.Z.A.A. The Impact of Substation Grounding Grid Design Parameters in Non-Homogenous Soil to the Grid Safety Threshold Parameters. *IEEE Access* **2021**, *9*, 37497–37509. [[CrossRef](#)]
58. Gouda, O.; Amer, G.; EL-Saied, T. Factors Affecting the Apparent Soil Resistivity of Multi-Layer Soil. In Proceedings of the XIVth International Symposium on High Voltage Engineering, Tsinghua University, Beijing, China, 25–29 August 2005; pp. 1–4.
59. Paramo, R.; Faleiro, E.; Asensio, G.; Moreno, J. Functionally Graded Multilayered Soil Models, an Alternative to Modeling the Soil Electrical Resistivity for Computing the Grounding Resistance. *IEEE Access* **2021**, *9*, 55364–55372. [[CrossRef](#)]
60. Zhu, L.; Jiang, H.; Yang, F.; Luo, H.; Li, W.; Han, J. Fem Analysis and Sensor-Based Measurement Scheme of Current Distribution for Grounding Electrode. *Appl. Sci.* **2020**, *10*, 8151. [[CrossRef](#)]
61. Mokhtari, M.; Abdul-Malek, Z.; Salam, Z. An Improved Circuit-Based Model of a Grounding Electrode by Considering the Current Rate of Rise and Soil Ionization Factors. *IEEE Trans. Power Deliv.* **2015**, *30*, 211–219. [[CrossRef](#)]

62. Zeng, R.; He, J.; Gao, Y.; Zou, J.; Guan, Z. Grounding Resistance Measurement Analysis of Grounding System in Vertical-Layered Soil. *IEEE Trans. Power Deliv.* **2004**, *19*, 1553–1559. [[CrossRef](#)]
63. Rancic, P.D. Analysis of Linear Ground Electrodes Placed in Vertical Three-Layer Earth. *IEEE Trans. Magn.* **1996**, *32*, 1505–1508. [[CrossRef](#)]
64. Ramos-Leanos, O.; Uribe, F.A.; Valcarcel, L.; Hajiaboli, A.; Franiatte, S.; Dawalibi, F.P. Nonlinear Electrode Arrangements for Multilayer Soil Resistivity Measurements. *IEEE Trans. Electromagn. Compat.* **2020**, *62*, 2148–2155. [[CrossRef](#)]
65. Markovski, B.; Grcev, L.; Arnautovski-Toseva, V. Fast and Accurate Transient Analysis of Large Grounding Systems in Multilayer Soil. *IEEE Trans. Power Deliv.* **2021**, *36*, 598–606. [[CrossRef](#)]
66. Li, Z.X.; Yin, Y.; Wang, K.C. Lightning Response of a Grounding System Buried in Multilayered Earth Based on the Galerkin's Boundary Element and Quasi-Static Complex Image Methods. *IEEE Trans. Electromagn. Compat.* **2021**, 1–10. [[CrossRef](#)]
67. Nayel, M.; Lu, B.; Tian, Y.; Zhao, Y. Study of Soil Resistivity Measurements in Vertical Two-Layer Soil Model. In Proceedings of the 2012 Asia-Pacific Power and Energy Engineering Conference, Shanghai, China, 27–29 March 2012; pp. 1–5. [[CrossRef](#)]
68. Zeng, R.; He, J.; Gao, Y.; Sun, W.; Su, Q. Measuring Electrode Arrangement for Grounding Resistance Measurement of Grounding System in Vertical-Layered Soil. In Proceedings of the PowerCon 2000. 2000 International Conference on Power System Technology. Proceedings (Cat. No.00EX409), Perth, Australia, 4–7 December 2000; pp. 1469–1474. [[CrossRef](#)]
69. Pavel, S.G.; Maier, V.; Ciorca, C.; Beleiu, H.G.; Birou, I. Optimal Design of the Vertical Earthing with Electrodes Arranged in Line. *Appl. Sci.* **2020**, *10*, 1177. [[CrossRef](#)]